Sensors & Actuators: B. Chemical 375 (2023) 132895

Contents lists available at ScienceDirect

Sensors and Actuators: B. Chemical

journal homepage: www.elsevier.com/locate/snb

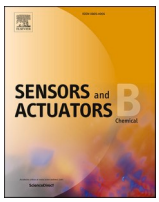

Carbon nanodots modified-electrode for peroxide-free cholesterol biosensing and biofuel cell design

Melisa del Barrio [a,b,*], Emiliano Martínez-Periñán [a], Cristina Gutiérrez-Sánchez [a], Eva Mateo-Martí [c], Marcos Pita [b], Antonio L. De Lacey [b], Félix Pariente [a], Encarnación Lorenzo [a,d,*]

[a] Departamento de Química Analítica y Análisis Instrumental, Universidad Autónoma de Madrid, Ciudad Universitaria de Cantoblanco, 28049 Madrid, Spain
[b] Instituto de Catálisis y Petroleoquímica, CSIC, C/ Marie Curie 2, 28049 Madrid, Spain
[c] Centro de Astrobiología (CSIC-INTA), Ctra. Ajalvir, Km. 4, Torrejón de Ardoz, 28850 Madrid, Spain
[d] IMDEA-Nanociencia, Ciudad Universitaria de Cantoblanco, 28049 Madrid, Spain

ARTICLE INFO

Keywords:
Carbon nanodots
Dehydrogenase
Cholesterol
Biosensor
Biofuel cell

ABSTRACT

The determination of cholesterol is greatly important because high concentrations of this biomarker are associated to heart disease. Moreover, cholesterol can be used as a fuel in enzymatic fuel cells operating under physiological conditions. Here, we present a cholesterol biosensor and a peroxide-free biofuel cell based on the electrocatalytic oxidation of the NADH generated during the enzymatic reaction of cholesterol dehydrogenase (ChDH) as an alternative to the H_2O_2 biosensing strategies used with cholesterol oxidase-bioelectrodes. Azure A functionalized-carbon nanodots were used as NADH oxidation electrocatalysts and for ChDH covalent immobilization. The biosensor responded linearly to cholesterol concentrations up to 1.7 mM with good sensitivity (4.50 mA cm^{-2} M^{-1}) and at a low potential. The ChDH bioelectrode was combined with an O_2-reducing bilirubin oxidase cathode to produce electrical energy using cholesterol as fuel and O_2 as oxidant. Furthermore, the resulting enzymatic fuel cell was tested in human serum naturally containing free cholesterol.

1. Introduction

Cholesterol is the most common steroid lipid and an essential structural component of animal cell membranes. It is also an important biomarker because high blood cholesterol levels are linked to ischemic heart disease, atherosclerosis, and stroke, among other diseases [1–4]. In general, total cholesterol in blood should be below 5 mM, although for patients with cardiovascular disorders or diabetes the levels should be lower (4.5 mM) [5]. Adequate monitoring of cholesterol can help to prevent and assess the risk of developing cardiovascular disease, as well as to control high cholesterol treatments. The simple and rapid measurements that biosensors can provide are clearly advantageous over the classical methods for cholesterol determination, such as the Liebermann-Burchard test, which employs corrosive reagents, or chromatographic techniques, which require complex procedures and costly equipment [3,6,7]. In the present context, research on technologies for more effective, affordable and sustainable biosensors is of paramount importance.

The current status of enzymatic detection of cholesterol with point-of-care devices as well as the advances in ultrasensitive electrochemical biosensors for cholesterol have been reviewed recently [3,8]. Electrochemical cholesterol biosensors have achieved high success and a few have been marketed (e.g. CardioChek "Cholesterol & Glucose Test Monitors" by Polymer Technology Systems Inc. (PS-003528 ER1 1005)) [7]. Most electrochemical biosensors are based on the enzyme cholesterol oxidase (ChOx) that catalyzes the oxidation of cholesterol to cholest-3-ene-4-one using oxygen as electron acceptor with the subsequent formation of H_2O_2. The measurement of cholesterol is performed by the quantification of H_2O_2 at the electrode [9–12]. Apart from ChOx, a biosensor based on cytochrome P450scc [13] and, more recently, a bioelectrode having immobilized cholesterol dehydrogenase (ChDH) and diaphorase in a bilayer fashion [14] have been reported. ChDH also catalyzes the oxidation of cholesterol, but it uses nicotineamide adenine dinucleotide (NAD^+) as electron acceptor instead of O_2, generating

* Corresponding authors at: Departamento de Química Analítica y Análisis Instrumental, Universidad Autónoma de Madrid, Ciudad Universitaria de Cantoblanco, 28049 Madrid, Spain.
E-mail addresses: melisa.delbarrio@csic.es (M. del Barrio), encarnacion.lorenzo@uam.es (E. Lorenzo).

https://doi.org/10.1016/j.snb.2022.132895
Received 15 July 2022; Received in revised form 23 September 2022; Accepted 22 October 2022
Available online 25 October 2022

NADH (the reduced form of the redox couple) and not H_2O_2. This difference is advantageous since biosensors using the dehydrogenase enzyme are independent of O_2 availability, thus variable O_2 concentration in samples does not affect their reproducibility. NADH can be oxidized by using electrocatalysts that lower the oxidation overpotential at carbon electrode surfaces and therefore minimize the interferences from compounds present in biological samples, whereas H_2O_2 detection methods are prone to interferences [14]. Various NADH oxidation catalysts, such as quinone derivatives, phenazines, phenothiazines, nitro-fluorenone and catechol, have been extensively studied [15–18] due to the ubiquity of the enzymatic reactions involving NADH as a cofactor and therefore the relevance of NADH detection. Furthermore, the grafting of phenazines and phenothiazines on screen printed electrodes for NADH oxidation has been reported [18–20].

Most biosensors require a power source to operate, e.g. a battery. However, lithium batteries raise environmental concerns, are difficult to miniaturize and complicate the sensor design [21]. Enzymatic fuel cells constitute a potential solution to these issues, as they enable the production of electrical energy under mild conditions by using physiological fluids as the fuel [22]. Generally, oxidoreductase enzymes are used as biocatalysts for fuel oxidation at the anode, and multicopper oxidases (laccase and bilirubin oxidase) or peroxidase catalyze the reduction of O_2 or peroxides, respectively, to H_2O at the cathode [22–24]. These electrochemical devices have an extremely simple design of only two electrodes (the anode and the cathode) and open the possibility to develop autonomous biosensors, in which the power output correlates to the analyte concentration [25]. Although research on autonomous systems has been focused mainly on glucose, lactate and ethanol self-powered biosensors [25–29], other biomarkers such as acetylcholine and cholesterol have been also considered [21,30,31]. A single-enzyme self-powered biosensor for free cholesterol based on ChOx and Prussian blue was reported by Sekretaryova et al. [32]. This is the only cholesterol self-powered biosensor reported to date, in which the short-circuit current response is proportional to the analyte concentration.

Among the latest carbon-based nanomaterials, carbon nanodots (CNDs) are particularly interesting due to their excellent solubility, biocompatibility, low cost and sustainable synthetic procedures [33–35]. Very recently, we have functionalized CNDs with dyes acting as redox or optical probes by insertion of the probe in the CNDs structure in a single-step synthetic procedure [36,37]. This modification strategy is simpler than those including post-synthetic modifications of CNDs. In the present work, we functionalized CNDs with Azure A, a phenothiazine dye which is known to catalyze the oxidation of NADH [18], and for the first time, we electrografted the modified nanomaterial on an electrode surface for the development of an enzymatic biosensor.

Here, we present a cholesterol biosensor based on the electrocatalytic oxidation of the NADH generated during the enzymatic reaction of cholesterol dehydrogenase (Scheme 1A) as an alternative to the H_2O_2 biosensing strategies used with cholesterol oxidase-bioelectrodes. Azure A functionalized-carbon nanodots were used as NADH oxidation electrocatalysts and for ChDH covalent immobilization. The bioelectrode was combined with an O_2-reducing bilirubin oxidase (BOx) cathode (Scheme 1B) to produce electrical energy using cholesterol as fuel and O_2 as oxidant. The resulting enzymatic fuel cell (EFC) was characterized and tested in human serum naturally containing free cholesterol.

2. Materials and methods

2.1. Chemicals

L-arginine, 3,3′-diamino-N-methyldipropylamine, Azure A (AA), morpholine ethanesulphonic acid (MES) hydrate, disodium hydrogen phosphate, sodium dihydrate phosphate, potassium ferricyanide, potassium ferrocyanide trihydrate, N-(3-(dimethylamino)propyl)-ethyl-carbodiimide hydrochloride (EDC), N-hydroxysuccinimide (NHS), sodium nitrite, cholesterol dehydrogenase (ChDH) from *Nocardia* species (33.8 U mg^{-1}), bilirubin oxidase (BOx) from *Myrothecium verrucaria* (9.1 U mg^{-1}), cholesterol, β-nicotinamide adenine dinucleotide (NAD^+), β-nicotinamide adenine dinucleotide reduced disodium salt hydrate (NADH) and human serum (from human male AB plasma, USA origin, sterile-filtered) were purchased from Merck. Dialysis membrane tubing, 100–500 Da cut-off, was provided by Spectrum Laboratories. Multiwall carbon nanotubes (MWCNTs) were provided by Nanocyl S.A. Triton X-100, hydrochloric acid and N,N-dimethyl formamide (DMF) were purchased from Scharlau. All solutions were prepared using MilliQ water purified with a Millipore Milli-Q-System station (18.2 MΩ cm at 25 ºC). Cholesterol is minimally soluble in water. Homogeneous cholesterol solutions were prepared as reported in [38]: A stock 10 mM cholesterol solution was prepared in phosphate buffer (0.1 M, pH = 7.5) containing 10 % (w/w) of Triton X-100 in a thermostated bath at 65 °C. This solution was stored at 4 °C in the dark and was stable for at least 15 days (until turbidity was observed).

2.2. Instrumentation

A microwave system CEM Discover (Matthews (NC), USA) was used for AA-CNDs synthesis. A Cary Eclipse Varian spectrofluorimeter was used for fluorescence measurements. UV-Vis spectra were recorded

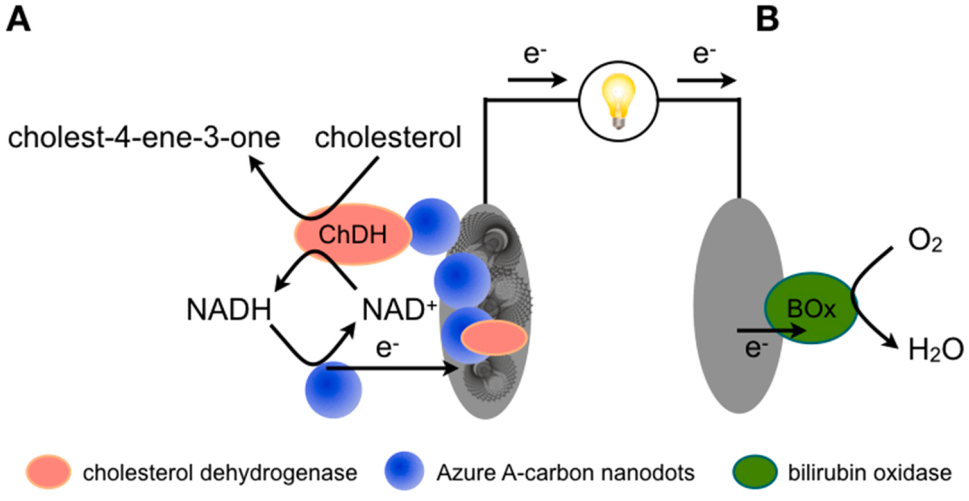

Scheme 1. (A) Cholesterol biosensor (bioanode) and (B) O_2-reducing biocathode coupled in an enzymatic fuel cell configuration.

using a UV-1900 spectrophotometer from SHIMADZU using a quartz cell. Lacey carbon support film copper grids (400 mesh, Electron Microscopy Sciences) were employed for transmission electron microscopy (TEM). A JEOL JEM 2100 electron microscope was used for this purpose. Elemental analysis of Azure A modified carbon nanodots (AA-CNDs) was performed with Perkin-Elmer 2400 CHN elemental analyzer.

Electrochemical measurements were conducted with an Autolab potentiostat PGSTAT 30 from Metrohm. Experiments were performed in a three-electrode cell configuration using a Pt wire as a counter electrode and an Ag/AgCl (3 M NaCl) reference electrode at room temperature. The cell was filled with 2 mL of 100 mM phosphate buffer pH 7.4 containing 2.5 % (w/w) Triton X-100. The presence of Triton X-100 is required for the enzymatic oxidation of cholesterol by cholesterol dehydrogenase. The surfactant acts as an enzyme activator [39]. The biofuel cell was characterized by linear sweep voltammetry at 1 mVs^{-1}, starting at the OCP initially recorded. A porous frit was used to separate the biocathode from the buffer solution containing the surfactant for preventing the loss of BOx activity. All potentials mentioned in the manuscript are referred vs. Ag/AgCl unless otherwise stated.

2.3. Azure A-carbon nanodots (AA-CNDs) synthesis

AA-CNDs were synthesized following a similar procedure to that reported in [37] using a different mediator. 87 mg of L-arginine, 73 mg of Azure A, 86 μL of 3,3′-diamino-N-methyldipropylamine and 100 μL Milli-Q water were mixed and then irradiated in a microwave system at a constant temperature of 240 ºC and at a maximum pressure of 20 bar for 3 min. The obtained solid was dispersed in 10 mL of ultra-pure water and filtered using a 0.1 μm porous filter. The suspension was then dialyzed in a 100–500 Da dialysis membrane for 1 week. The final concentration of as prepared AA-CNDs was 2.0 mg mL^{-1}. The resulting AA-CNDs suspension was stored at 4 ºC until use. Unmodified CNDs (without AA) were also prepared by using the same procedure without adding AA to the precursors mixture [40].

2.4. Preparation of the AA-CNDs/ChDH-modified bioanode

Glassy carbon (GC) electrodes (BASi-Bioanalytical Systems, Inc.; diameter = 3 mm) were polished with 1 μm diamond paste (Buehler) and rinsed with water and ethanol. 10 μL of a 1 mg MWCNTs suspension in DMF, previously sonicated for 30 min, were dropcasted on the GC electrode surface and dried at 70 ºC. AA-CNDs were diazotated in an ice bath by mixing 500 μL of the AA-CNDs suspension and 500 μL of 60 mM $NaNO_2$ in HCl (0.5 M) during 45 min. The grafting of AA-CNDs on the electrode surface was performed by immersing the GC/MWCNTs electrodes in the previous solution and cycling the potential between 0.5 V and − 1 V at 0.10 V/s to electrochemically reduce the in situ generated diazonium salt. 10 reductive scans were performed to improve the catalytic efficiency for NADH oxidation (it was about 40% higher than that after 2 scans). Non-diazotated AA-CNDs were prepared in a 0.25 M HCl solution (without $NaNO_2$). The electrografting of AA in the absence of CNDs was also performed for the analysis of the catalytic NADH oxidation. The concentration of AA was equivalent to that present in AA-CNDs and was calculated from the S content obtained by elemental analysis ([Azure A] = 337 μM). The resulting modified electrodes were washed with purified water before experiments or further modifications. Cholesterol dehydrogenase was covalently immobilized on AA-CNDs-modified electrodes by the carbodiimide method: 3.6 μL of ChDH (81 mg mL^{-1}), 1.2 μL of 14 mM EDC and 1.2 μL of 21 mM NHS, in pH 6 MES buffer (10 mM), were deposited on the electrode surface and incubated for 90 min. Afterwards the modified electrode was rinsed with pH 6 MES buffer and used for the electrochemical measurements.

2.5. Determination of cholesterol human serum

The concentration of free cholesterol in human serum was determined by the standard addition method in a sample spiked with increasing concentrations of cholesterol (from 0.1 mM to 1 mM) containing 10 mM NAD^+ and 2.5 % Triton X-100.

2.6. Preparation of the biocathode

BOx was immobilized on low density graphite (LDG) electrodes according to a previously reported method [41]. LDG rods of 3 mm diameter (Merck) were immersed into an electrochemical cell filled with an ice-cooled solution, prepared immediately before its use by mixing 5 mL of 20 mM 6-amino-2-naftoic acid in acetonitrile and 5 mL of 2 mM $NaNO_2$ in 2 M HCl aqueous solution. Two reductive cyclic voltammograms from 0.6 V to − 0.3 V at 0.200 $V{\cdot}s^{-1}$ were recorded. After rinsing the electrode with water, 20 μL of 0.83 $mg{\cdot}mL^{-1}$ BOx in 10 mM MES buffer pH 6 were deposited on the electrode surface and covered with a lid to avoid evaporation for 30 min. Afterwards, covalent immobilization was performed by adding 5 μL of 36 mM EDC and 5 μL of 17 mM NHS, both in 10 mM MES buffer pH 6, and left to react for 90 min at room temperature.

3. Results

3.1. Characterization of AA-CNDs and AA-CNDs-modified bioanodes

AA-CNDs were characterized by different techniques to investigate their morphology and composition. Fig. 1A shows the TEM micrographs of the spherical AA-CNDs. The determined mean diameter, after measuring around 150 particles at different TEM images, was 2.8 ± 0.8 nm (Fig. 1B). All AA-CNDs had a diameter in the range between 1.0 and 5.5 nm.

UV-Vis absorption spectroscopy also showed relevant information regarding the structure of the nanomaterial (Fig. 1C). AA-CNDs spectrum (blue line) exhibits an absorption peak at 285 nm due to the π-π * transition of the conjugated C═C. This kind of groups are normally present in the core of carbon nanodots. The same band has been detected in the unmodified carbon nanodots spectrum (black line). The contribution observed in the AA-CNDs spectrum at 300 nm is ascribed to the π-π * transition of the phenothiazine ring as it can be also detected in the AA spectrum (red line). In the AA spectrum, the band at 635 nm is related to the n–π * transitions of the C– = N bond of the phenothiazine ring. In the case of AA-CNDs, this contribution appears as a broad band with two peaks at 560 and 614 nm. This different behavior between AA and AA-CNDs is a consequence of the covalent bond stablished in AA molecules when they are inserted (covalently) in the carbon nanodots structure. Another evidence that supports the covalent link of the Azure A phenothiazine ring in the carbon nanodots structure was revealed by fluorescence spectroscopy. As shown in the fluorescence spectrum in Fig. 1D, AA-CNDs (blue), unmodified CNDs (black) and Azure A (red) solutions emit radiation at 360 nm upon 300 nm excitation. However, the fluorescence emission intensity is higher in the case of AA-CNDs compared with unmodified CNDs and AA (in equivalent concentrations). We attribute this effect to the presence of AA molecules covalently linked to the carbon nanodots structure.

Elemental analysis of AA-CNDs and unmodified CNDs were carried out to detect differences in the composition of the new synthesized nanomaterial. In the case of AA-CNDs the obtained results were 52.58 % C, 8.12 % H, 20.78 % N, 1.44 % S and 17.08 % O (calculated by subtraction). The data obtained for unmodified carbon nanodots were 50.29 % C, 9.04 % H, 21.93 % N, 0.00 % S and 18.74 % O (calculated by subtraction). The presence of S in AA-CNDs can be considered an evidence of the insertion of the phenothiazine, since S is not found in the unmodified CNDs.

Further characterization of AA-CNDs using FTIR and XPS was carried out showing the covalent insertion of AA molecules into the carbon nanodots nanostructure. The main bands observed at the FT-IR spectrum (Fig. 1E) of AA-CNDs (blue line) are the same as those observed in the

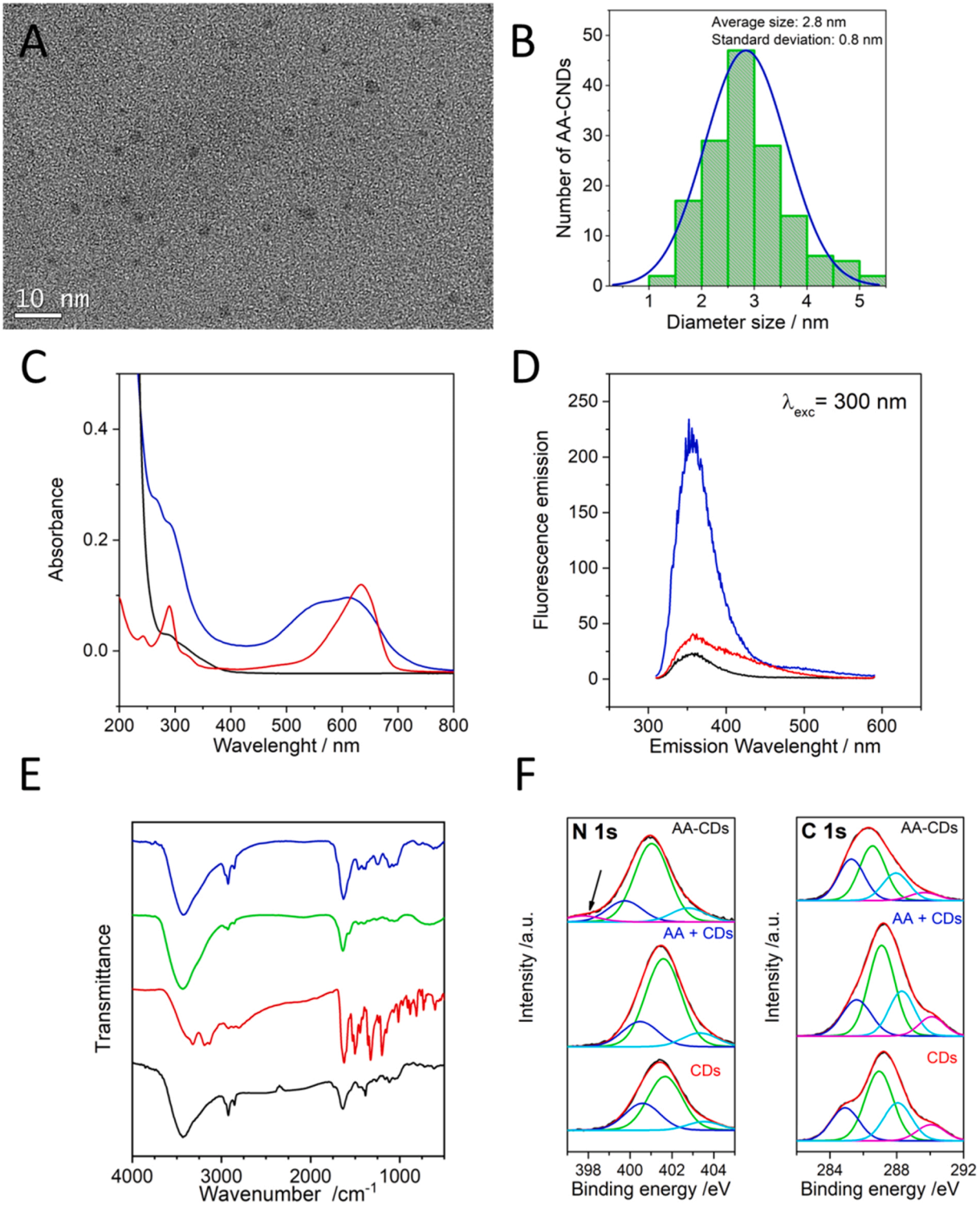

Fig. 1. (A) TEM micrograph of synthesized AA-CNDs and (B) AA-CNDs size histogram obtained from measuring 150 particles. (C) UV–Vis spectra and (D) fluorescence emission spectra (λexc = 300 nm) of 0.11 mg·mL^{-1} of AA-CNDs (blue), 0.11 mg·mL^{-1} of CNDs (black) and 10 μM AA (red) in Milli-Q water. (E) FT-IR spectra of AA-CNDs (blue), CNDs (black), AA (red) and a mixture of CNDs and molecular AA (AA+CNDs) (green). (F) XPS N 1s and C 1s regions of AA-CNDs, CNDs and AA+CNDs.

unmodified CNDs spectrum (black line): the bands at 1639 and 896 cm^{-1}, corresponding to primary amines, and the band at 802 cm^{-1}, ascribed to secondary amines, are all of them due to the L-arginine precursor; whereas the bands at 3432, 1639 and 1116 cm^{-1} (primary amines) and the band at 1166 cm^{-1} (tertiary amine) come from the 3,3′-diamino-N-methyldipropylamine. The bands in the AA-CNDs spectrum (blue line) that are in agreement with the presence of AA molecules are those at 1654, 1500 and 1203 cm^{-1}, related to tertiary amines and secondary aromatic amines, respectively, and which are similar bands to those detected in the AA spectrum (red line). Furthermore, the band around 1628 cm^{-1} is attributed to N-H bending, which agrees well with the insertion of phenothiazine rings in the AA-CNDs nanostructure

rather than a simple adsorption happening when an equivalent amount of AA is adsorbed over unmodified carbon nanodots (AA+CNDs) (green line).

XPS analysis of AA-CNDs, AA+CNDs and CNDs samples was also performed to confirm the successful insertion of AA in AA-CNDs. Fig. 1F shows the N 1s and C 1s core level peaks of the three samples. The high-resolution spectrum of nitrogen, which shows complex features, was carefully decomposed. The best fit of the N 1s core level shows three contributions at about 400.0–400.5 eV, 401.1–401.66 eV and 403.0–403.5 eV, which are assigned to nitrogen in N-(C3), C═N (cycles) and N═C positively charged quaternary species, respectively [42]. The AA-CNDs exhibit an additional forth nitrogen component at 397.9 eV, which could be attributed to the pyridinic nitrogen (imine) [42–44], i.e., to nitrogen with a lone electron pair, located either at the edge of the graphitic network or next to a vacancy, and bonded to two carbon atoms. The presence of this additional component only for AA-CNDs (it does not appear in the AA+CNDs sample, without covalent linkage) suggests a chemical structure modification, compatible with a covalent interaction between the AA dye and the CNDs. Therefore, these data confirm the insertion of AA in the carbon nanodots (AA-CNDs), which does not occur in the AA+CNDs mixture. Moreover, the C 1s peak of the AA-CNDs shows significant changes compared to CNDs and AA+CNDs (see Fig. 1F, C 1s). Although the C 1s core level peak shows four similar components for AA-CNDs, AA+CNDs and CNDs samples, at 285.2 eV, 286.8 eV, 288.2 eV and 289.9 eV, the ratio between the intensity of the components differs for AA-CNDs. AA-CNDs show a noteworthy increase in the first carbon component; CNDs and AA+CNDs show however a very similar peak profile in the carbon region. This corroborates the chemical structure modification indicated above for AA-CNDs.

In previous works, we have demonstrated that the aromatic primary amine groups of CNDs can be diazotated to form a covalent bond onto carbon conductive surfaces by an electrografting process [40,45]. Here, AA-CNDs were electrografted for the first time on GC/MWCNTs electrodes to obtain a stable modified surface capable of electrocatalysing NADH oxidation. When cycling the potential as described in the experimental section, a cathodic process ascribed to the reduction of aryldiazonium groups in CNDs was observed (Fig. S1A). This process generates highly reactive aryl radicals that can be grafted on the electrode surface forming C-C bonds. To discriminate if the electrografting was performed via diazonium groups generated from the CNDs amino groups or of the AA ones, a solution containing a similar concentration of the dye to that in the modified CNDs (estimated through the S content in AA-CNDs) was submitted to the same electrografting procedure (Fig. S1B). The reduction process observed during the AA-CNDs electrografting is similar to that reported for unmodified CNDs containing amino groups [40,45], whereas the electrochemical processes detected when AA was employed, which are characteristic of the electrografting of AA on carbon conductive surfaces [18], were not detected when AA-CNDs were electrografted. This suggests that the immobilization of the AA-CNDs was mainly performed through the diazotated amine groups of the CNDs. Control experiments using non-diazotated AA-CNDs did not show reduction processes (Fig. S1C). These results confirm the diazotation and reduction of the aromatic amines in AA-CNDs, resulting in a covalent attachment of the modified CNDs on GC/MWCNTs electrodes.

The covalent immobilization of AA-CNDs on the GC/MWCNTs electrode was studied by means of AFM. Fig. 2A shows an AFM topographic image of a GC surface after modification with MWCNTs followed by the AA-CNDs electrografting procedure. It is observed that the surface is completely covered with a film mainly formed of globular structures randomly distributed along the surface. Fig. 2B shows the GC/MWCNTs surface in the absence of AA-CNDs. As can be seen, the surface is completely covered, but not in a homogeneous way because there are areas less covered with MWCNTs. Figs. 2D and 2E represent the topographic profile of both surfaces, GC/MWCNTs/AA-CNDs and GC/MWCNTs. Significant differences are observed in the profiles, showing that in the case of the GC/MWCNTs surface there are bare areas. These results suggest that surface modification with AA-CNDs is effective. AA-

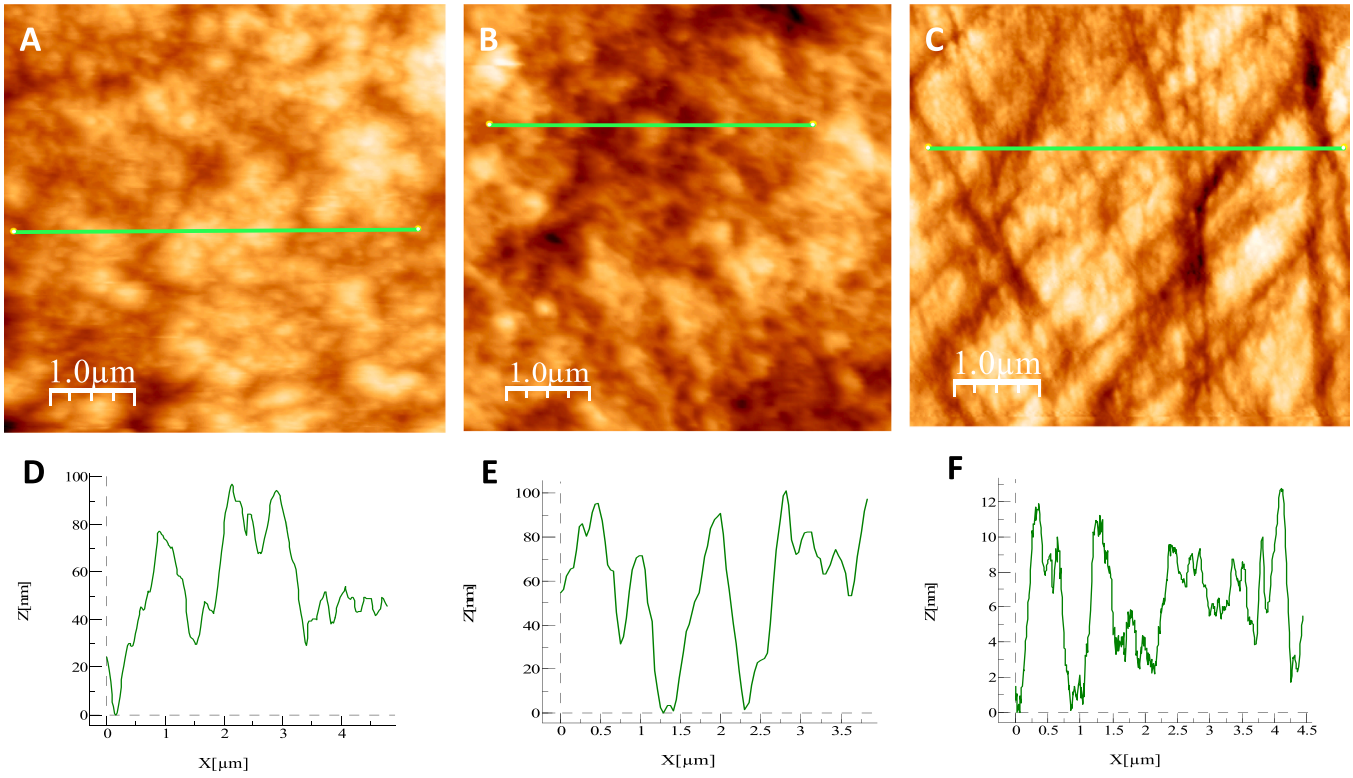

Fig. 2. AFM topographic images of GC/MWCNTs/AA-CNDs (A), GC/MWCNTs (B) and GC (C). Associated topographic profile plotted as a line in Figure A, B and D, respectively (D, E and F).

CNDs are electrografted on the electrode surface, completely covering the entire surface in a homogeneous and compact manner. As a control, the AFM image of the GC electrode without modification and its corresponding profile can be seen in Figs. 2C and 2F.

We also characterized the electrodes after the surface modification steps by cyclic voltammetry in the presence of the ferri/ferrocyanide redox couple. GC, GC/MWCNTs, GC/MWCNTS/AA-CNDs and GC/MWCNTS/AA-CNDs/ChDH electrodes were analysed. Fig. S2 and Table S1 show that the electrochemical signal considerably improves after modification of the GC surface with MWCNTs: the peak current intensities (i_{pa}, i_{pc}) of ferricyanide/ferrocyanide increase, whereas peaks separation (ΔE) decreases. This effect is explained by the increase of the electroactive area and the enhancement of the electron transfer kinetics of the redox probe. Further modification with AA-CNDs and ChDH do not significantly improve the electrochemical response. These results support that the modification of the GC electrode surface performed by dropcasting of MWCNTs was required for efficient electrografting of AA-CNDs and sensitive cholesterol biosensing. The higher sensitivity and stability of biosensors based on MWCNTs dropcasted on carbon electrodes has been often reported before [46,47] and confirm strong adsorption of MWCNTs on GC.

3.2. Electrocatalytic oxidation of NADH on the AA-CNDs-modified electrode

The oxidation of NADH on AA-CNDs-modified electrodes was investigated by cyclic voltammetry experiments in the absence and in the presence of the surfactant Triton X-100 (Fig. 3), which is required for cholesterol solubilization and substrate oxidation by cholesterol dehydrogenase. The oxidation current at ca. − 0.050 V ascribed to the mediator Azure A in AA-CNDs increased upon NADH addition (Fig. 3A). A 60 mV-shift towards higher potentials was observed for the peak potential when the surfactant was added, whereas the peak current barely changed. As can be seen by comparison with Figs. 3B and 3C, AA-CNDs decrease the overpotential of NADH oxidation in a larger extent than AA or MWCNTs in the presence of Triton X-100; the overpotentials required at GC/MWCNTs/AA and GC/MWCNTs electrodes are, respectively, 100 mV and 400 mV higher than that on AA-CNDs modified electrodes. In contrast to the small effect of Triton X-100 in the electrochemical response obtained with AA-CNDs-modified electrodes, the surfactant strongly affects the NADH oxidation in the absence of AA-CNDs; GC/MWCTs and AA-modified electrodes showed a 200 mV-shift towards more oxidant potentials and the electrocatalytic current of AA remarkably decreased.

The NADH oxidation peak currents obtained with AA-CNDs-modified electrodes at various scan rates increase linearly with the scan rate (peak current (μA) = 0.45 (mVs^{-1}) + 3.5; R^2 = 0.999, Fig. S3), suggesting that the electrocatalytic oxidation is an adsorption-controlled process. Even though the adsorption of the NAD^+/NADH species occurs on the electrode surface, the AA-CNDs-modified electrodes are barely affected by passivation as it will be demonstrated by the results shown in Section 3.3 (the catalytic response is stable after several measurements).

3.3. Determination of cholesterol

The AA-CNDs-modified electrodes were combined with ChDH for the determination of cholesterol. An increase in the oxidation catalytic current was observed in voltammetry experiments after the addition of cholesterol, indicating that the NADH generated by the enzyme during the oxidation of the substrate is re-oxidized by the electrocatalytic AA-CNDs system (Fig. S4A). The results of control experiments in the absence of the enzyme (Fig. S5) demonstrate that the AA-CNDs modified electrodes do not respond to cholesterol, meaning that the presence of the enzyme is required for cholesterol sensing. In addition, the immobilization of ChDH on AA-modified electrodes without CNDs did not lead to an electrochemical response after cholesterol addition.

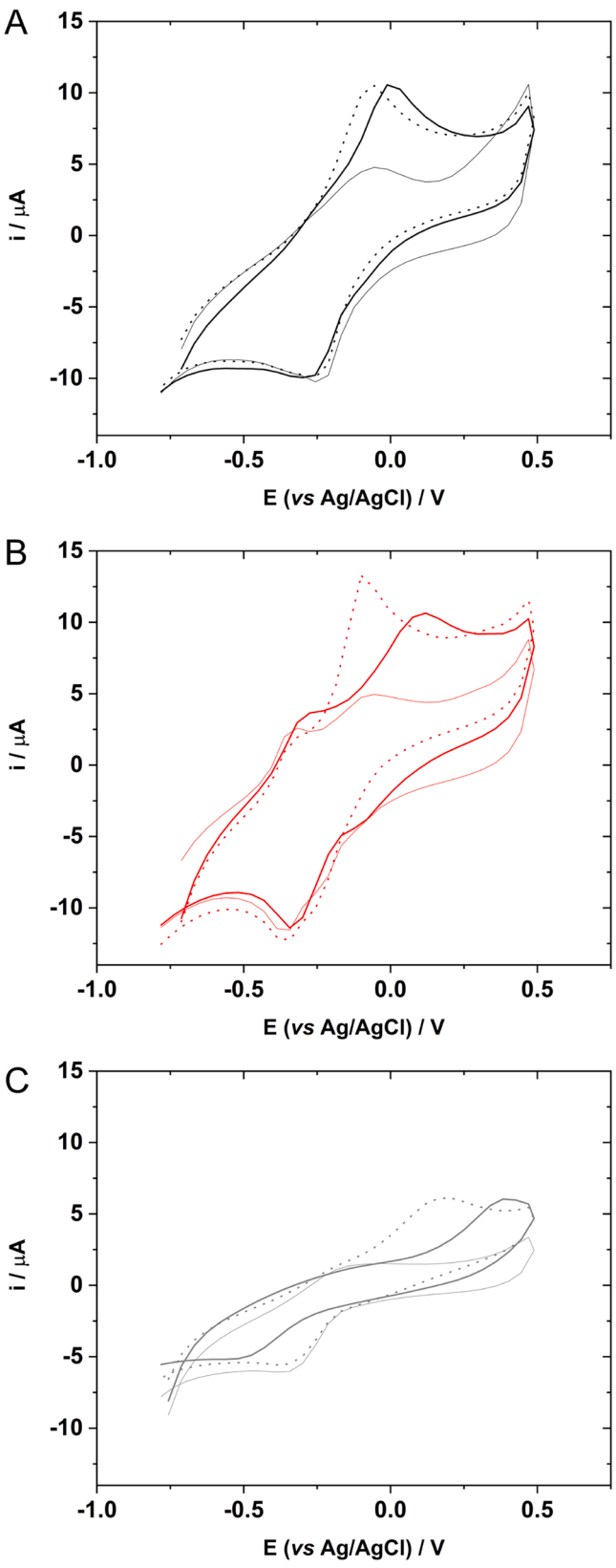

Fig. 3. Electrocatalytic oxidation of NADH on GC/MWCNTs electrodes with (A) electrografted AA-CNDs, (B) electrografted AA and (C) without additional modifications in the absence (dotted lines) and in the presence (thick lines) of Triton X-100. Cyclic voltammograms in thin lines were performed in the absence of NADH. Conditions: $\nu = 10$ mV/s, [NADH] = 1 mM, pH 7.5 phosphate buffer (100 mM), 2.5 % Triton X-100.

Therefore, CNDs are required for the attachment of the enzyme and for the subsequent detection of cholesterol.

Fig. 4A shows the amperometric response to increasing concentrations of cholesterol of AA-CNDs/ChDH-modified bioelectrodes containing 10 U of ChDH, poised at 0.2 V (vs Ag/AgCl, 3M Cl^-). Bioelectrodes prepared with lower amount of enzyme provided poor signal reproducibility (Fig. S6). As can be seen in Fig. 4A, the current density (j) transients stabilized after a few seconds and their values increased with cholesterol concentration in the range measured according to the Michaelis-Menten model (Fig. 4B). The apparent Michaelis-Menten constant, K_M^{app}, was 2.9 ± 0.6 mM. This value is higher than that reported with a bioanode based on ChDH [14]. Nevertheless, the lower affinity of our bioanode broadens the linear range for the determination of cholesterol. The calibration plot (inset to Fig. 4B), obtained with 3 independent electrodes, depicted a linear range between 0.1 and 1.7 mM (current density (μA cm^{-2}) = 4.50 [Cholesterol] (mM) – 0.006; R^2 = 0.992). A sensitivity of 4.5 ± 0.4 mA cm^{-2} M^{-1} was obtained. The detection and determination limits were calculated to be 1.0 μM and 2.6 μM. The reproducibility was evaluated for the determination of 1 mM cholesterol using 3 different electrodes (RSD: 9.6 %). The evaluation of the stability of the sensor showed that 86 % of the signal obtained with a 1 mM cholesterol solution was retained after 24 h and more than 10 determinations. The electrode was stored in buffer solution between measurements.

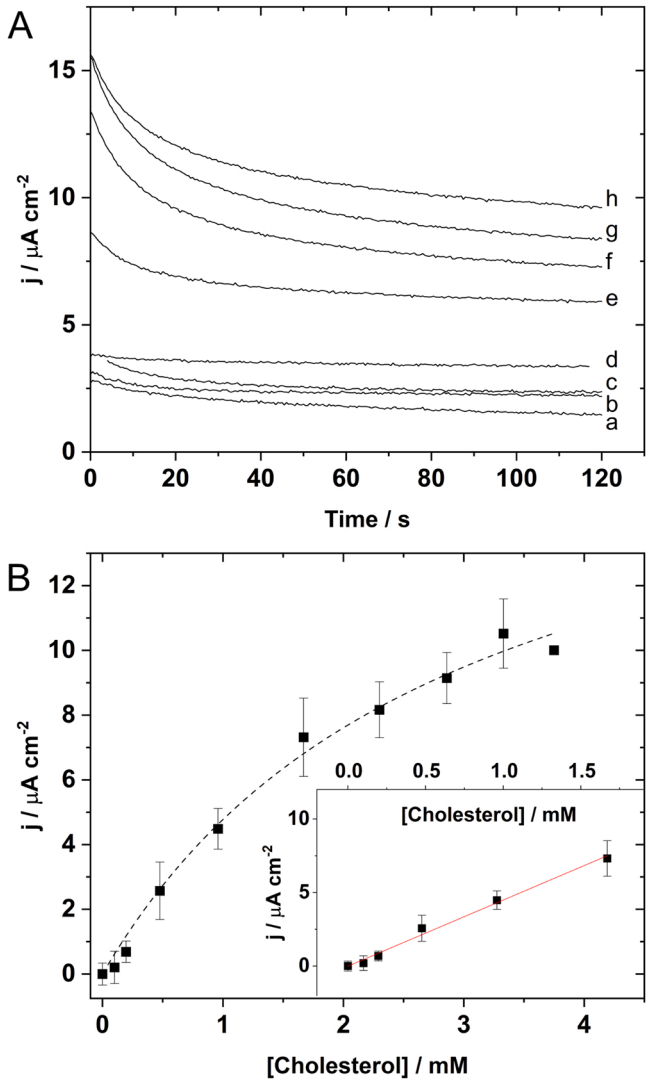

Fig. 4. (A) Chronoamperometric response of the AA-CNDs/ChDH-modified bioelectrode towards cholesterol (a: blank; b: 0.1 mM; c: 0.2 mM; d: 0.5 mM; e: 1.0 mM; f: 1.7 mM; g: 2.3 mM; h: 3.8 mM). (B) Dependence of the current density on cholesterol concentration. The dashed line is the non-linear regression for the calculation of K_M^{app}. Inset: Calibration plot (current density (μA cm^{-2}) = 4.50 [Cholesterol] (mM) - 0.006; R^2 = 0.992; n = 3 electrodes). Conditions: E = 0.2 V vs Ag/AgCl (3 M Cl^-), pH 7.5 phosphate buffer (100 mM), 2.5 % Triton X-100, [NAD^+] = 10 mM.

To the best of our knowledge, only two bioelectrodes for cholesterol determination based on ChDH have been reported before: a disposable biosensor for total (free and esterified) cholesterol [48] and a bioanode for (free) cholesterol which uses an additional enzyme (diaphorase) in combination to ChDH [14]. Our biosensor has a simpler design with only one enzyme, works at lower potential, and responds linearly to free cholesterol in the physiological range (up to 1.7 mM), in contrast to the most sensitive bioelectrode (Table 1). The normal range of total cholesterol is from 4.14 mM to 5.18 mM, approximately a range of free cholesterol from 1.24 mM to 1.55 mM (30 % of total).

3.4. Interference study

The effect of various potential interfering compounds in the electrochemical response of AA-CNDs/ChDH-modified bioelectrodes was evaluated in the presence of 1.7 mM cholesterol. The variations in the current density values at 0.2 V are inferior to 5 % for the compounds tested (Table 2). These results indicate that the developed biosensor can be used for the selective determination of cholesterol.

3.5. Analysis of cholesterol in human serum

The concentration of free cholesterol in human serum was determined by the standard addition method as described in Materials and methods. A concentration of 1.0 mM free cholesterol was found. The certified concentration of total cholesterol in the sample is 3.6 mM, and accounts for free cholesterol and lipoproteins containing cholesterol. The concentration of free cholesterol is generally around 30 % of the total, thus 1.1 mM. This value is consistent with the concentration determined with the AA-CNDs/ChDH-modified electrodes (recovery = 93 %) indicating that the bioelectrodes are suitable for the determination of free cholesterol in real human serum.

3.6. Application to enzymatic fuel cell development

Given that cholesterol can be used as a fuel for EFCs operating under physiological conditions, the AA-CNDs/ChDH bioelectrode was combined with an O_2-reducing BOx cathode to produce electrical energy.

Table 1
Comparison of the analytical characteristics of cholesterol bioelectrodes based on ChDH.

Electrode	Sensitivity (mA cm^{-2} M^{-1})	Linear range (mM)	Detection limit (μM)	E vs Ag/AgCl (V)	Refs.
Screen printed carbon/working ink:1,10-phenanthroline-5,6-dione/ChDH/NAD/cholesterol esterase	9.1[a]	1.29 – 12.88[a]	386[a]	0.3[b]	[48]
Toray carbon paper/$FcMe_2$-LPEI/diaphorase/C_8-LPEI/ChDH	60.12	0.005 – 0.2	5	0.34	[14]
GC/MWCNTS/AA-CNDs/ChDH	4.5	0.1 – 1.7	1	0.2	This work

[a] Data refers to esterified cholesterol. [b] Potential vs carbon pseudo-reference electrode.

Table 2
Effect of interferent compounds in the electrochemical response of AA-CNDs/ChDH-modified bioelectrodes in the presence of 1.7 mM cholesterol.

Interferents	Concentration	Current density variation
Glucose	10 mM	+ 2 %
Uric acid	100 μM	< 1 %
K^+	10 mM	-5 %
Na^+	10 mM	+ 1 %
Acetaminophen	1 mM	< 1 %

The BOx biocathode undergoes the 4e$^-$ reduction of O_2 to H_2O at high potential without the need of a mediator [23]. This is expected to increase the open-circuit potential (OCP) of the EFC. Furthermore, the inhibition of BOx by H_2O_2, which affects the stability of ECFs employing oxidases, is not problematic in our case since this compound is not produced at the ChDH bioelectrode [14,49].

The voltammetric characterization of the biocathode shows a reduction wave with an onset potential of 0.5 V and a maximum catalytic current of about 17 μA, whereas the catalytic current of the bioanode is lower than that of the biocathode and increases at − 0.1 V (Fig. S4). This indicates that the bioanode is the rate-limiting electrode.

Fig. 5 shows the power and current density curves of the assembled EFC that couples the AA-CNDs/ChDH bioanode and the BOx biocathode. The short-circuit current density and the maximum power density (P_{max}) in buffer containing 10 mM NAD^+ and 2.5 mM cholesterol were 38 μA cm^{-2} and 3.8 μW cm^{-2} at 0.25 V, respectively. The open circuit potential (OCP) was 0.493 ± 0.012 V (n = 3), which corresponds well with the difference between the bioanode and the biocathode potentials. The obtained OCP is higher than that of the only reported cholesterol self-powered biosensor based on cholesterol oxidase [32] and similar to that achieved with the only other EFC employing ChDH [14]. These results demonstrate the potential of our system for the development of self-powered biosensors in which the power generated by the EFC sustains sensor operation.

The performance of the EFC was evaluated at different cholesterol concentrations by applying 0.25 V. The power density linearly increased in the cholesterol range from 0.9 to 2.9 mM (R^2 = 0.996) (Fig. S7).

The EFC was also tested in human serum naturally containing cholesterol (3.6 mM total cholesterol, approximately 1.1 mM free cholesterol) supplemented with 10 mM NAD^+ and 2.5 % Triton X-100 (Fig. 5B). A P_{max} of 1.57 μW cm^{-2} at 0.25 V, a short-circuit current density of 19 μA cm^{-2} and an OCP of 470 mV were reached. Although the OCP of the EFC was hardly unaltered in human serum, a decrease in the power density was observed. This lower power density could be due to the presence of compounds in human serum (e.g., proteins) that foul the electrode as well as redox-active species.

4. Conclusions

We have developed a cholesterol biosensor based on the electrocatalytic oxidation of the NADH generated during the enzymatic reaction of ChDH, as an alternative to cholesterol oxidase-bioelectrodes that detect H_2O_2. This biosensing strategy is not limited by O_2 availability and facilitates the design of enzymatic fuel cells, as H_2O_2 is an inhibitor of enzymes frequently used at the biocathode. The ChDH bioelectrodes modified with Azure A-carbon nanodots allow the determination of free cholesterol in the physiological range with good sensitivity, reproducibility and at low potential. In combination with a BOx biocathode, we demonstrated the production of electrical energy under physiological conditions in using the cholesterol naturally present in human serum as a fuel and O_2 as an oxidant. These results contribute to the development of self-powered cholesterol biosensors independent of oxygen availability and therefore with improved reproducibility.

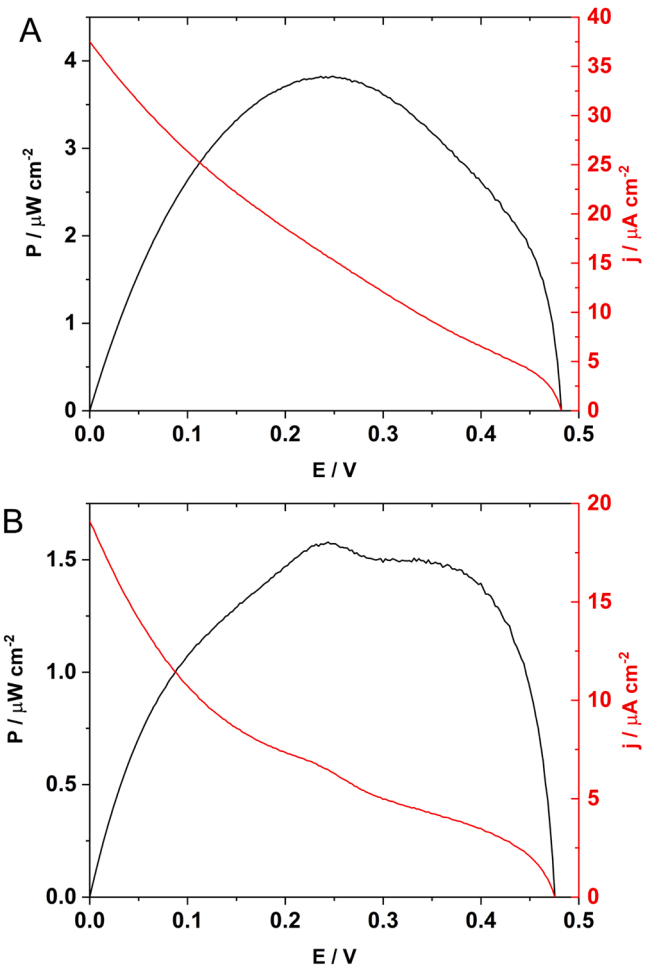

Fig. 5. Power density (black) and current density (red) curves of the EFC obtained (A) in 2.5 mM cholesterol and (B) in human serum. Conditions: pH 7.5 phosphate buffer (100 mM), 2.5% Triton X-100, [NAD^+] = 10 mM.

CRediT authorship contribution statement

Melisa del Barrio: Conceptualization, Investigation, analysis, Writing – review and editing, Funding acquisition; **Emiliano Martínez-Periñán**: Investigation, Writing; **Cristina Gutiérrez-Sánchez**: Investigation, Writing, Funding acquisition; **Eva Mateo-Martí** : Investigation; **Marcos Pita**: Supervision, review; **Antonio L. De Lacey**: Supervision, review, Funding acquisition; **Félix Pariente**: Supervision; **Encarnación Lorenzo**: Supervision, review, Funding acquisition.

Declaration of Competing Interest

The authors declare that they have no known competing financial interests or personal relationships that could have appeared to influence the work reported in this paper.

Data availability

Data will be made available on request.

Acknowledgments

A.L.DL. and M.P. thank MCIU/AEI/FEDER, EU for funding project RTI2018–095090-B-I00. M.B. acknowledges funding from the European Union's Horizon 2020 Research and Innovation Program under the Marie Skłodowska-Curie grant agreement No. 713366. This work was

also supported by Talent Attraction Project from CAM (SI3/PJI/2021–00341 and 2021–5A/BIO-20943), Spanish Ministerio de Ciencia e Innovacion (PID2020–116728RB-I00) and TRANSNANOAVANSENS-CAM Program (S2018/NMT-4349).

Appendix A. Supporting information

Supplementary data associated with this article can be found in the online version at doi:10.1016/j.snb.2022.132895.

References

[1] C.J. Murray, J.A. Lauer, R.C. Hutubessy, L. Niessen, N. Tomijima, A. Rodgers, C. M. Lawes, D.B. Evans, Effectiveness and costs of interventions to lower systolic blood pressure and cholesterol: a global and regional analysis on reduction of cardiovascular-disease risk, Lancet 361 (2003) 717–725, https://doi.org/10.1016/S0140-6736(03)12655-4.

[2] P. Libby, J.E. Buring, L. Badimon, G.K. Hansson, J. Deanfield, M.S. Bittencourt, L. Tokgözoğlu, E.F. Lewis, Atherosclerosis, Nat. Rev. Dis. Prim. 5 (2019) 56, https://doi.org/10.1038/s41572-019-0106-z.

[3] X. Wang, L. Hu, Review – enzymatic strips for detection of serum total cholesterol with point-of-care testing (POCT) devices: current status and future prospect, J. Electrochem. Soc. 167 (2020), 037535, https://doi.org/10.1149/1945-7111/ab64bb.

[4] W.M.M. Verschuren, D.R. Jacobs, B.P.M. Bloemberg, D. Kromhout, A. Menotti, C. Aravanis, H. Blackburn, R. Buzina, A.S. Dontas, F. Fidanza, M.J. Karvonen, S. Nedelijković, A. Nissinen, H. Toshima, Serum total cholesterol and long-term coronary heart disease mortality in different cultures: twenty-five—year follow-up of the seven countries study, JAMA 274 (1995) 131–136, https://doi.org/10.1001/jama.1995.03530020049031.

[5] G. De Backer, E. Ambrosioni, K. Borch-Johnsen, C. Brotons, R. Cifkova, J. Dallongeville, S. Ebrahim, O. Faergeman, I. Graham, G. Mancia, V.M. Cats, K. Orth-Gomér, J. Perk, K. Pyörälä, J.L. Rodicio, S. Sans, V. Sansoy, U. Sechtem, S. Silber, T. Thomsen, D. Wood, C. Albus, N. Bages, G. Burell, R. Conroy, H. Christian Deter, C. Hermann-Lingen, S. Humphries, A. Fitzgerald, B. Oldenburg, N. Schneiderman, A. Uutela, R. Williams, J. Yarnell, S.G. Priori, M. Angeles Alonso Garcia, J.-J. Blanc, A. Budaj, M. Cowie, V. Dean, J. Deckers, E. Fernández Burgos, J. Lekakis, B. Lindahl, G. Mazzotta, K. McGregor, J. Morais, A. Oto, O. Smiseth, H.-J. Trappe, A. Budaj, C.-D. Agardh, J.-P. Bassand, J. Deckers, M. Godycki-Cwirko, A. Heagerty, R. Heine, P. Home, S. Priori, P. Puska, M. Rayner, A. Rosengren, M. Sammut, J. Shepherd, J. Siegrist, M. Simoons, M. Tendera, A. Zanchetti, European guidelines on cardiovascular disease prevention in clinical practice: third joint task force of European and other societies on cardiovascular disease prevention in clinical practice (constituted by representatives of eight societies and by invited experts), Eur. Heart J. 24 (2003) 1601–1610, https://doi.org/10.1016/S0195-668X(03)00347-6.

[6] J. MacLachlan, A.T.L. Wotherspoon, R.O. Ansell, C.J.W. Brooks, Cholesterol oxidase: sources, physical properties and analytical applications, J. Steroid Biochem. Mol. Biol. 72 (2000) 169–195, https://doi.org/10.1016/S0960-0760(00)00044-3.

[7] S.K. Arya, M. Datta, B.D. Malhotra, Recent advances in cholesterol biosensor, Biosens. Bioelectron. 23 (2008) 1083–1100, https://doi.org/10.1016/j.bios.2007.10.018.

[8] N. Thakur, D. Gupta, D. Mandal, T.C. Nagaiah, Ultrasensitive electrochemical biosensors for dopamine and cholesterol: recent advances, challenges and strategies, Chem. Commun. 57 (2021) 13084–13113, https://doi.org/10.1039/D1CC05271C.

[9] J. Shen, C.-C. Liu, Development of a screen-printed cholesterol biosensor: comparing the performance of gold and platinum as the working electrode material and fabrication using a self-assembly approach, Sens. Actuators B: Chem. 120 (2007) 417–425, https://doi.org/10.1016/j.snb.2006.02.035.

[10] Md.M. Rahman, X. Li, J. Kim, B.O. Lim, A.J.S. Ahammad, J.-J. Lee, A cholesterol biosensor based on a bi-enzyme immobilized on conducting poly(thionine) film, Sens. Actuators B: Chem. 202 (2014) 536–542, https://doi.org/10.1016/j.snb.2014.05.114.

[11] G. Kaur, M. Tomar, V. Gupta, Development of a microfluidic electrochemical biosensor: prospect for point-of-care cholesterol monitoring, Sens. Actuators B: Chem. 261 (2018) 460–466, https://doi.org/10.1016/j.snb.2018.01.144.

[12] N. Ruecha, R. Rangkupan, N. Rodthongkum, O. Chailapakul, Novel paper-based cholesterol biosensor using graphene/polyvinylpyrrolidone/polyaniline nanocomposite, Biosens. Bioelectron. 52 (2014) 13–19, https://doi.org/10.1016/j.bios.2013.08.018.

[13] V. Shumyantseva, G. Deluca, T. Bulko, S. Carrara, C. Nicolini, S.A. Usanov, A. Archakov, Cholesterol amperometric biosensor based on cytochrome P450scc, Biosens. Bioelectron. 19 (2004) 971–976, https://doi.org/10.1016/j.bios.2003.09.001.

[14] T. Quah, S. Abdellaoui, R.D. Milton, D.P. Hickey, S.D. Minteer, Cholesterol as a promising alternative energy source: bioelectrocatalytic oxidation using NAD-dependent cholesterol dehydrogenase in human serum, J. Electrochem. Soc. 164 (2017) H3024–H3029, https://doi.org/10.1149/2.0021703jes.

[15] N. Mano, A. Thienpont, A. Kuhn, Adsorption and catalytic activity of trinitro-fluorenone derivatives towards NADH oxidation on different electrode materials, Electrochem. Commun. 3 (2001) 585–589, https://doi.org/10.1016/S1388-2481(01)00224-7.

[16] A. Maleki, D. Nematollahi, J. Clausmeyer, J. Henig, N. Plumeré, W. Schuhmann, Electrodeposition of catechol on glassy carbon electrode and its electrocatalytic activity toward NADH oxidation, Electroanalysis 24 (2012) 1932–1936, https://doi.org/10.1002/elan.201200251.

[17] L. Gorton, E. Domínguez, Electrocatalytic oxidation of NAD(P)H at mediator-modified electrodes, Rev. Mol. Biotechnol. 82 (2002) 371–392, https://doi.org/10.1016/S1389-0352(01)00053-8.

[18] M. Revenga-Parra, C. Gómez-Anquela, T. García-Mendiola, E. Gonzalez, F. Pariente, E. Lorenzo, Grafted Azure A modified electrodes as disposable β-nicotinamide adenine dinucleotide sensors, Anal. Chim. Acta 747 (2012) 84–91, https://doi.org/10.1016/j.aca.2012.07.043.

[19] B. Doumèche, L.J. Blum, NADH oxidation on screen-printed electrode modified with a new phenothiazine diazonium salt, Electrochem. Commun. 12 (2010) 1398–1402, https://doi.org/10.1016/j.elecom.2010.07.031.

[20] S. Abdellaoui, M. Bekhouche, A. Noiriel, R. Henkens, C. Bonaventura, L.J. Blum, B. Doumèche, Rapid electrochemical screening of NAD-dependent dehydrogenases in a 96-well format, Chem. Commun. 49 (2013) 5781–5783, https://doi.org/10.1039/C3CC42065E.

[21] C. Gonzalez-Solino, M.D. Lorenzo, Enzymatic fuel cells: towards self-powered implantable and wearable diagnostics, Biosensors 8 (2018) 11, https://doi.org/10.3390/bios8010011.

[22] M. Rasmussen, S. Abdellaoui, S.D. Minteer, Enzymatic biofuel cells: 30 years of critical advancements, Biosens. Bioelectron. 76 (2016) 91–102, https://doi.org/10.1016/j.bios.2015.06.029.

[23] N. Mano, A. de Poulpiquet, O_2 reduction in enzymatic biofuel cells, Chem. Rev. 118 (2018) 2392–2468, https://doi.org/10.1021/acs.chemrev.7b00220.

[24] T. Ohara, M. Vreeke, F. Battaglini, A. Heller, Bienzyme sensors based on "electrically wired" peroxidase, Electroanalysis 5 (1993) 825–831.

[25] F. Conzuelo, A. Ruff, W. Schuhmann, Self-powered bioelectrochemical devices, Curr. Opin. Electrochem. 12 (2018) 156–163, https://doi.org/10.1016/j.coelec.2018.05.010.

[26] E. Katz, A.F. Bückmann, I. Willner, Self-powered enzyme-based biosensors, J. Am. Chem. Soc. 123 (2001) 10752–10753, https://doi.org/10.1021/ja0167102.

[27] M. Falk, M. Alcalde, P.N. Bartlett, A.L. De Lacey, L. Gorton, C. Gutierrez-Sanchez, R. Haddad, J. Kilburn, D. Leech, R. Ludwig, E. Magner, D.M. Mate, P.Ó. Conghaile, R. Ortiz, M. Pita, S. Pöller, T. Ruzgas, U. Salaj-Kosla, W. Schuhmann, F. Sebelius, M. Shao, L. Stoica, C. Sygmund, J. Tilly, M.D. Toscano, J. Vivekananthan, E. Wright, S. Shleev, Self-powered wireless carbohydrate/oxygen sensitive biodevice based on radio signal transmission, PLOS One 9 (2014) 1–9, https://doi.org/10.1371/journal.pone.0109104.

[28] M. Zhou, Recent progress on the development of biofuel cells for self-powered electrochemical biosensing and logic biosensing: a review, Electroanalysis 27 (2015), https://doi.org/10.1002/elan.201500173.

[29] A. Ruff, P. Pinyou, M. Nolten, F. Conzuelo, W. Schuhmann, A self-powered ethanol biosensor, ChemElectroChem 4 (2017) 890–897.

[30] F.T.C. Moreira, M.G.F. Sale, M. Di Lorenzo, Towards timely Alzheimer diagnosis: a self-powered amperometric biosensor for the neurotransmitter acetylcholine, Biosens. Bioelectron. 87 (2017) 607–614, https://doi.org/10.1016/j.bios.2016.08.104.

[31] L. Fu, J. Liu, Z. Hu, M. Zhou, Recent advances in the construction of biofuel cells based self-powered electrochemical biosensors: a review, Electroanalysis 30 (2018) 2535–2550.

[32] A.N. Sekretaryova, V. Beni, M. Eriksson, A.A. Karyakin, A.P.F. Turner, M. Yu Vagin, Cholesterol self-powered biosensor, Anal. Chem. 86 (2014) 9540–9547, https://doi.org/10.1021/ac501699p.

[33] S. Campuzano, P. Yáñez-Sedeño, J.M. Pingarrón, Carbon dots and graphene quantum dots in electrochemical biosensing, Nanomaterials 9 (2019), https://doi.org/10.3390/nano9040634.

[34] Z. Hassanvand, F. Jalali, M. Nazari, F. Parnianchi, C. Santoro, Carbon nanodots in electrochemical sensors and biosensors: a review, ChemElectroChem 8 (2021) 15–35, https://doi.org/10.1002/celc.202001229.

[35] L. Xiao, H. Sun, Novel properties and applications of carbon nanodots, Nanoscale Horiz. 3 (2018) 565–597, https://doi.org/10.1039/C8NH00106E.

[36] E. Martínez-Periñán, Á. Martínez-Sobrino, I. Bravo, T. García-Mendiola, E. Mateo-Martí, F. Pariente, E. Lorenzo, Neutral Red-carbon nanodots for selective fluorescent DNA sensing, Anal. Bioanal. Chem. (2022), https://doi.org/10.1007/s00216-022-03980-1.

[37] E. Martínez-Periñán, T. García-Mendiola, E. Enebral-Romero, R. del Caño, M. Vera-Hidalgo, M. Vázquez Sulleiro, C. Navío, F. Pariente, E.M. Pérez, E. Lorenzo, A MoS_2 platform and thionine-carbon nanodots for sensitive and selective detection of pathogens, Biosens. Bioelectron. 189 (2021), 113375, https://doi.org/10.1016/j.bios.2021.113375.

[38] J.-C. Vidal, J. Espuelas, E. Garcia-Ruiz, J.-R. Castillo, Amperometric cholesterol biosensors based on the electropolymerization of pyrrole and the electrocatalytic effect of Prussian-Blue layers helped with self-assembled monolayers, Talanta 64 (2004) 655–664, https://doi.org/10.1016/j.talanta.2004.03.038.

[39] K. Kishi, Y. Watazu, Y. Katayama, H. Okabe, The characteristics and applications of recombinant cholesterol dehydrogenase, Biosci. Biotechnol. Biochem. 64 (2000) 1352–1358, https://doi.org/10.1271/bbb.64.1352.

[40] T. Guerrero-Esteban, C. Gutiérrez-Sánchez, E. Martínez-Periñán, M. Revenga-Parra, F. Pariente, E. Lorenzo, Sensitive glyphosate electrochemiluminescence immunosensor based on electrografted carbon nanodots, Sens. Actuators B: Chem. 330 (2021), 129389, https://doi.org/10.1016/j.snb.2020.129389.

[41] C. Gutiérrez-Sánchez, M. Pita, M.D. Toscano, A.L. DeLacey, Bilirubin oxidase-based nanobiocathode working in serum-mimic buffer for implantable biofuel cell, Electroanalysis 25 (2013) 1359–1362, https://doi.org/10.1002/elan.201200668.
[42] M.J. Mostazo-López, R. Ruiz-Rosas, T. Tagaya, Y. Hatakeyama, S. Shiraishi, E. Morallón, D. Cazorla-Amorós, Nitrogen doped superactivated carbons prepared at mild conditions as electrodes for supercapacitors in organic electrolyte, C 6 (2020), https://doi.org/10.3390/c6030056.
[43] D. Liu, W. Lei, D. Portehault, S. Qin, Y. Chen, High N-content holey few-layered graphene electrocatalysts: scalable solvent-less production, J. Mater. Chem. A 3 (2015) 1682–1687, https://doi.org/10.1039/C4TA05008H.
[44] T. Susi, T. Pichler, P. Ayala, X-ray photoelectron spectroscopy of graphitic carbon nanomaterials doped with heteroatoms, Beilstein J. Nanotechnol. 6 (2015) 177–192, https://doi.org/10.3762/bjnano.6.17.
[45] C. Gutiérrez-Sánchez, M. Mediavilla, T. Guerrero-Esteban, M. Revenga-Parra, F. Pariente, E. Lorenzo, Direct covalent immobilization of new nitrogen-doped carbon nanodots by electrografting for sensing applications, Carbon 159 (2020) 303–310, https://doi.org/10.1016/j.carbon.2019.12.053.
[46] A. Geto, M. Pita, A.L. De Lacey, M. Tessema, S. Admassie, Electrochemical determination of berberine at a multi-walled carbon nanotubes-modified glassy carbon electrode, Sens. Actuators B: Chem. 183 (2013) 96–101, https://doi.org/10.1016/j.snb.2013.03.121.
[47] R.D. Crapnell, C.E. Banks, Electroanalytical overview: utilising micro- and nano-dimensional sized materials in electrochemical-based biosensing platforms, Mikrochim. Acta 188 (2021) 268, https://doi.org/10.1007/s00604-021-04913-y.
[48] C. Fang, J. He, Z. Chen, A disposable amperometric biosensor for determining total cholesterol in whole blood, Sens. Actuators B-Chem. 155 (2011) 545–550.
[49] R.D. Milton, F. Giroud, A.E. Thumser, S.D. Minteer, R.C.T. Slade, Bilirubin oxidase bioelectrocatalytic cathodes: the impact of hydrogen peroxide, Chem. Commun. 50 (2014) 94–96, https://doi.org/10.1039/C3CC47689H.

Melisa del Barrio obtained her Ph.D. in Analytical Chemistry from the University of Zaragoza in 2014. She held postdoctoral positions at CNRS in Toulouse and Marseille (France). She was a Marie Skłodowska-Curie Cofund fellow at Universidad Autónoma de Madrid and CSIC between 2019 and 2021. Her research activities have been interdisciplinary and are mainly focused on enzymatic sensors, bioelectrocatalysis, the development of analytical methodologies, and their application in biochemistry.

Emiliano Martínez-Periñán received his bachelor's degree and Master degree in chemistry from Universidad de Cádiz. He obtained his Ph.D. degree from Universidad Autónoma de Madrid in 2016. After that, he had been working as a visiting postdoc researcher at Manchester Metropolitan University under the direction of Professor Craig E. Banks. Then, he obtained a Juan de la Cierva-Formación fellowship from the Spanish Ministry of economy and innovation at the Electroanalysis and Electrochemical Biosensors group of Universidad Complutense de Madrid lead by Professor José Manuel Pingarrón. Nowadays he is working as associated professor in the department of Analytical Chemistry and Instrumental analysis of Universidad Autónoma de Madrid. He is part of the Chemical Sensors and Biosensors group lead by Professor Encarnación Lorenzo. His research interests include electrosynthesis, nanotechnology, the use of different analysis techniques coupled with electrochemistry and electrochemical sensors.

Cristina Gutiérrez-Sánchez received her PhD degree from UNED in 2012, in the Bioelectrocatalysis laboratory of the Institute of Catalysis, CSIC, under the direction of Dr. Antonio Lopez De Lacey. She worked on the functionalization and characterization of surfaces using different techniques for the development of nanostructured enzyme electrodes. In 2013, she undertook her first postdoctoral contract at the University of Siegen, Germany. Subsequently, she moved to Marseille, France, to the CNRS Bioenergetics and Protein Engineering laboratory, for 2 years. Later, she joined the Bioelectrocatalysis group at the Institute of Catalysis, CSIC in 2016. She is currently working in the group of Chemical Sensors and Biosensors at UAM to carry out the Research Project in the Call for Talent Attraction, modality 1 of the Community of Madrid. Her main research interests include areas as Analytical Chemistry, Bioelectrochemistry, Nanoscience and Materials Science.

Eva Mateo-Martí received her Ph.D. degree on surface science at Leverhulme Center for Innovative Catalysis, University of Liverpool (UK), Post-Doctoral at Ecole Nationale Superieure de Chimie de Paris (France), and currently permanent Scientific Researcher at Centro de Astrobiologia, Instituto Nacional de T é cnica Aeroespacial in Madrid (Spain). Her main expertize based on spectroscopies applied to surface science studies, planetary simulation chambers and ultra-high vacuum systems. She leads research on reactivity and preservation of biomolecules on surfaces, and its stability due to different environments, searching for spectroscopical fingerprints applied to prebiotic chemistry and planetary exploration. She is a co-author of more than 70 research articles in a wide range of international journals and three patents.

Marcos Pita achieved his Ph.D. at ICP-CSIC working from 2002 to 2006 on nanoparticle engineering for the biomolecule immobilization, where he also learned on bioelectrochemistry with laccase for O_2 reduction. Later he spent 3 years at Clarkson University (NY, USA) as a Post-doctoral Research Assistant with Prof. Evgeny Katz. The research focused on bioelectrochemical systems and enzyme biofuel cells. Year 2009 he obtained a Ramon y Cajal tenure-track contract, which allowed his reincorporation to ICP-CSIC early 2010. From 2010–2014 he developed his research at ICP-CSIC working on nanostructured materials for bioelectrochemical processes together with Prof. Victor Fernandez and Dr. Antonio L. De Lacey. He achieved his tenure incorporated in January 2015 Staff Researcher in Biocatalysis Department, ICP, where currently he is still working. Dr. Pita is author of over 100 scientific publications which have been cited 5000 times.

Antonio L. De Lacey received his Degree in Chemistry in 1989 from the Universidad Complutense de Madrid. He obtained his Ph.D. in Chemistry from the Universidad Autónoma de Madrid in 1995, working under the supervision of Prof. V. M. Fernandez at the Instituto de Catálisis (CSIC). From 1996–1998 he was a Marie Curie postdoctorate at CNRS/Université de Tecnologie de Compiegne, France. Since 2002 he is a permanent Researcher at the Instituto de Catálisis (CSIC). His research interests are focused on metalloenzyme structure/function relationships, bioelectrocatalysis and electrode modification for biosensor, biofuel cells, photocatalysis and cofactor regeneration applications.

Félix Pariente is Full Professor of Analytical Chemistry at the Universidad Autónoma de Madrid (UAM). He was born in Madrid in 1954. He received his B.S. and Ph.D. degrees in Chemistry in 1976 and 1988, respectively. Between 1992 and 1996 he spent several periods as visiting scientist at the University of Cornell in USA. In 1998 he obtains the degree of permanent assistant professor in the UAM. The research carried out by Prof. Pariente has been focused on the design and characterization of different types of biosensors to determine analytes of interest, especially pollutants and biomarkers. As a result of this scientific activity 117 papers have been published, all of them in indexed scientific journals included in the Science Citation Index. Most of these papers are placed in the first third of the category of their area of knowledge according to their impact index (IP). Since the research carried out has had a multidisciplinary nature, the works have been published in journals assigned to different areas of knowledge. Some with very high IP such as Nano Letters (1), Development, Journal of Physical Chemistry or Nanoscale, among others. As a consequence of all these publications, the estimated h-index of Prof. Pariente is 34, according to the ISI Web of Knowledge.

Encarnación Lorenzo is currently Full Professor in the Department of Analytical Chemistry and Instrumental Analysis at the Universidad Autónoma de Madrid. She received her degree in Chemistry in 1978 and her Ph.D. degree in 1985 from the Universidad Autónoma de Madrid. Afterwards, she made a post-doctoral stage at the Department of Chemistry at Dublin City University. In 1990 she was visiting scientist (NATO Program) to the Department of Chemistry in Cornell University. In 1998 the members of the faculty of Tokio University of Agriculture and Technology invited her as visiting professor to the Department of Applied Chemistry. Actually, she is member of management committee of the Spanish Analytical Chemistry Society. Her research interest is the development of sensors and biosensors for the detection of analytes of environmental, clinical and food interest. She is the author/coauthor of more than 100 original research publications and several book chapters in the area of analytical chemistry.